Verification of the PMCEPT Monte Carlo dose Calculation Code for Simulations in Medical Physics

Oyeon Kum

School of Electrical Engineering and Computer Science
Kyungpook National University, Daegu, Korea

The parallel Monte Carlo electron and photon transport (PMCEPT) code [Kum and Lee, J. Korean Phys. Soc. 47, 716 (2006)] for calculating electron and photon beam doses has been developed based on the three dimensional geometry defined by computed tomography (CT) images and implemented on the Beowulf PC cluster. Understanding the limitations of Monte Carlo codes is useful in order to avoid systematic errors in simulations and to suggest further improvement of the codes. We evaluated the PMCEPT code by comparing its normalized depth doses for electron and photon beams with those of MCNP5, EGS4, DPM, and GEANT4 codes, and with measurements. The PMCEPT results agreed well with others in homogeneous and heterogeneous media within an error of 1~3% of the dose maximum. The computing time benchmark has also been performed for two cases, showing that the PMCEPT code was approximately twenty times faster than the MCNP5 for 20-MeV electron beams irradiated on the water phantom. For the 18-MV photon beams irradiated on the water phantom, the PMCEPT was three times faster than the GEANT4. Thus, the results suggest that the PMCEPT code is indeed appropriate for both fast and accurate simulations.

Key Words: PMCEPT code, Monte Carlo, Homogeneous and heterogeneous phantoms, Normalized depth dose, Computing time benchmark

INTRODUCTION

A Monte Carlo algorithm simulates the transport of particles from first-principles physics and accounts in a natural way for an electronic nonequilibrium at medium interfaces.[1] Combining first principles physics with realistic descriptions of the radiation source and patient target, the Monte Carlo transport method has the potential to calculate dose accurately over a wide variety of treatment delivery and patient conditions.[2] More accurate dose distributions should allow physicians to make better clinical planning decisions, once the more accurate doses are correlated with clinical knowledge. The prevalence of three dimensional planning systems such as computer-controlled multileaf collimators and other technologies has led to the increasing use of conformal and intensity modulated treatment.[3] Dose escalation studies using conformal fields require the ability to accurately correlate clinical outcome with dose and dose-volume information.[4] The value of such comparisons is questionable if the dose information is only approximate, and comparisons may have to be repeated when more accurate algorithms become available.

Due to the massive increase in computing power per unit cost in the last half century, the Monte Carlo technique has become ubiquitous in medical physics over the last half century with a doubling of papers on the subject every five years beginning with the first Physics in Medicine & Biology paper in 1967 until 2000, when the numbers leveled off.[5] The general purpose Monte Carlo codes currently in distribution are EGS,[6] ETRAN,[7] GEANT,[8] MCNP,[9] PENELOPE,[10] ITS,[11] and FLUKA.[12] These codes generally meet the basic accuracy requirements of radiotherapy, although many have limitations as well. However, they are too slow to use for routine treatment planning. To address this problem, several codes have been developed recently more specifically for use

This work was supported by KOSEF-MOST (No. M20706000007-07M0600-00710).
Submitted November 26, 2007, Accepted March 4, 2008
Corresponding Author: Oyeon Kum, School of Electrical Engineering and Computer Science, Kyungpook National University, Daegu 702-701, Korea.
Tel: 053)950-7324, Fax: 053)950-5505
Email: okum@knu.ac.kr

in radiation therapy, for example, MCDOSE,[13] VMC++,[14] XVMC,[15] MCPAT,[16] MMC,[17] DPM,[18] PEREGRINE,[2] and super Monte Carlo.[19] They reduced the computing times in the patient-dependent part of the problem through approximations or compromises including modified electron transport, limited tracking of low probability events, voxel-based transport methods, etc. Some are freely accessible and some are grant-based codes. However, there are a lot of problems in developing a customized cancer radiation treatment planning simulation system[20] with off-the-shelf codes. Thus, to develop a new code is a better policy for this purpose. We developed a parallel Monte Carlo electron and photon transport (PMCEPT)[21-23] code based on the standard message passing interface (MPI)[24] to meet clinically acceptable time limits. Careful validation and study for the new algorithm, however, is required.

Comparisons of the Monte Carlo particle transport code with benchmark experiments and with other codes are important to evaluate the accuracy of the calculated results.[25] Different mathematical algorithms and physical models used in the codes may lead to significantly erroneous results, even though all other systematic and statistical errors may be small. Thus, it is essential that a potential user be aware of all limitations of a code that arise either because of a different algorithm or a particular physical model used in the code. There have been a number of publications comparing a specific Monte Carlo code calculation with measured data and/or with other Monte Carlo codes for a number of Monte Carlo codes. However, many people still believe that full sets of verification experiments have not yet been completed for any of these codes, and much work remains to be done in this area.[26] Because of an increasing need for the benchmarking and quality assurance of the computer codes, a computational benchmarking initiative was proposed recently to develop rigorous benchmarking procedures, to compile the existing benchmark results, to design new benchmarks, and to implement the benchmark initiative in a collaborative manner.[27]

In this paper, we present such benchmark results. We have performed extensive benchmark tests by comparing the PMCEPT results with those of experiments and calculations from the MCNP5, EGS4, DPM, and GEANT4 codes. Comparison between the PMCEPT and the MCNP5 codes for high energy electron beams of 20-MeV irradiating on the water phantom was performed. The results agreed well with each other. Moreover, the calculation time benchmark result showed that the PMCEPT code was approximately twenty times faster than the MCNP5 code. Comparisons between the PMCEPT and the GEANT4 codes for high energy photon beams of 6- and 18-MV irradiating both water and beryllium phantoms were performed. The PMCEPT code was three times faster than the GEANT4 for the 18-MV photon beams. Comparisons between the PMCEPT and EGS4 and DPM were also performed for high energy electron beams ranging from 10- to 20-MeV irradiation on homogeneous and heterogeneous phantoms. Computing time benchmarks with EGS4 and DPM were not possible because we cite their results from their paper.[18] For further validation of the PMCEPT code, comparisons of the PMCEPT results with absolute calorimetric dose measurements for approximately 0.5- and 1.0-MeV electron beams incident on homogeneous and multilayered media were also performed. Overall, the PMCEPT results agreed well with others in homogeneous and heterogeneous media, with a maximum of 3% error. Section II gives a brief overview of the physical and computational models for coupled photon and electron/positron transport. Comparisons of the dose calculations are given in Section III. Finally, Section IV offers the conclusions of this study.

OVERVIEW OF THE PMCEPT TRANSPORT

The Boltzmann equation, an integro-differential equation that was derived by Ludwig Boltzmann in 1872 to study the properties of gases, applies equally well to a description of the behavior of radiation comprised of energetic photons and charged particles.[28] The Boltzmann equation is a continuity equation in phase space, which is made up of the three space coordinates of Euclidian geometry, the momentum, and the direction of a particle. This integro-differential equation is prohibitively complicated, not allowing for an analytical treatment except under severe approximations for radiation transport problems. The Monte Carlo method is the only available technique so far that can solve the equation without further approximations. Moreover, the transport behavior of the particle in matter is an inherently stochastic process that can

be described completely in statistical terms. Thus, the Monte Carlo method only simulates the transport of particles from first principles. Specifically, it is the most rigorous approach for dose calculations in three-dimensional heterogeneous media because it can account in a natural way for the electronic nonequilibrium at medium interfaces. Since a detailed description of the physical and the computational models has been given in reference 21, only a brief overview will be given in this paper.

1. Physical model

The PMCEPT code, a general Monte Carlo code, embodies physical reality by following a trajectory, with particles being created according to the distribution described by the source. Particles travel to a collision distance determined by a probability distribution that depends on the total cross section and then scatter into another energy and/or direction according to the corresponding differential cross-section. New secondary particles can be born while the primary particle interacts with the medium. These secondary particles are also transported in the same way. This procedure continues until all particles are absorbed or leave the region under consideration. Essentially, there are twelve possible processes by which the electromagnetic field of a photon may interact with matter. The four most important interactions are Compton scattering, pair production, photoelectric absorption, and Rayleigh scattering. The rest are negligible processes. The PMCEPT code includes these four primary scattering processes. Pair production is closely related to bremsstrahlung, and its cross section formulae are taken from the article by Motz, Olson, and Koch.[29] Some ideas from Butcher and Messel for mixing the cross sections for sampling of secondary spectra are used.[30] For kinetic energy equal to or below 50-MeV, the Born approximation cross sections are used, and the extreme relativistic Coulomb-corrected cross sections are used for 50-MeV and above. Photoelectric absorption is a mechanism by which the photon disappears and charged particles are ejected from the surrounding atoms. The atoms, left in excited states with vacancies in the ionized shells, may relax via the emission of fluorescent photons and Auger and Coster-Kronig electrons. For incident photon energies below the K-shell binding energy, the entire photon energy is deposited locally. The K-shell binding energy is always subtracted from the energy of the electron set in motion, even though there is a certain probability that the photon absorption process will take place with a shell other than the K-shell. The total photoelectric cross-sections are taken from Storm and Israel.[31] In Compton scattering, an incident photon is scattered by a loosely bound or virtually free electron. This process is considered an inelastic scattering in that some of the initial kinetic energy of the photon is needed in order to overcome the binding energy of the electron to the atom and, therefore, does not appear as the kinetic energy of the secondaries. The differential and total Compton-scattering cross-sections are taken from a formula originally due to Klein and Nishina.[32] Rayleigh scattering, also called electron resonance scattering, is an atomic process in which the incident photon is absorbed by a bound electron. This electron is raised to a higher energy state, and a second photon at the same energy level as the incident photon is then emitted, with the electron returning to its original state (therefore, it is not an excitation). In effect, the photon is scattered by the atomic electron cloud, with the entire atom recoiling. The photon undergoes only a slight change in its direction and incurs only an insignificant decrease in energy because of the small recoil energy absorbed by the atom. This process is considered to be elastic. The total cross-sections for this process are taken from Storm and Israel.[31]

A charged particle moving through a medium interacts with it basically in three different ways depending on its kinetic energy and the distance of the particle from the atom with which it interacts: (1) by collision with an atom as a whole, (2) by collision with an electron, and (3) by radiative processes (bremsstrahlung). When the distance of closest approach to the atom is large compared with the atomic dimensions, the moving charged particle interacts with the atom as a whole. The Coulomb force is the primary interaction force, resulting in an excitation or ionization of the atom. This distance encounter, sometimes called a soft collision, is described by either single or multiple elastic scattering. A single elastic scattering simulation is an event-by-event simulation of electron transport, which is often not possible due to limitations in computing power because of the large number of interactions with surrounding matter. To

overcome this difficulty, Berger[33] developed the condensed history technique, called multiple scattering. This idea is equivalent to solving a diffusion problem. Lewis[34] showed the exact solution by solving an integro-differential diffusion equation, which led to expressions for the various moments of the spatial and the angular distributions. The multiple scattering algorithm implemented in the PMCEPT code solves the Lewis[34] equations. If the distance of closest approach to the atom is of the order of the atomic dimensions, the moving charged particle interacts with one of the atomic electrons. This interaction results in the ejection of an electron from the atom with considerable energy: Møller scattering for an electron and Bhabha scattering for a positron. In general, the energy transmitted to the secondary electron is large compared to the binding energy, and the process can be treated as a free electron collision, but the intrinsic magnetic moment (spin) of the charged particle must be taken into account in the collision probability. In particular, when the two particles are identical, exchange phenomena occur and become important if the minimum distance of approach is of the order of the deBroglie wavelength, $\lambda = h/p$, where h is Planck's constant and p is the momentum.

When the high-energy charged particle pierces the electron clouds of an atom and approaches close to the nucleus of the atom, the electric field of the nucleus strongly defects the particle. This defection process results in radiative energy loss and the emitted radiation (bremsstrahlung) covers the entire energy spectrum up to the maximum kinetic energy of the charged particle. The review article by Koch and Motz[35] drives the basic formulae for this process. We also add the Butcher and Messel's idea[30] for mixing the cross-sections for sampling of the secondary spectra. When a charged particle travels through a condensed medium, it loses energy both via the hard collisions explained above and via an average stopping power effect (soft-collision term). The collision and radiative stopping power and the range tables are taken from the National Institute of Science and Technology (NIST) website[36] and the widely accepted International Commission of Radiation Units and Measurements (ICRU) tabulations.[37] To describe the soft-collision energy loss process, we use the continuous-slowing-down-approximation (CSDA), which is assumed to be equal to the stopping power. In this approximation, fluctuations in the energy loss are disregarded, and the energy of the particle is taken to be a deterministic function of the path-length traveled.

2. Parallel computational model

Since the Monte Carlo method is inherently parallel due to the independent nature of particle transport, the use of parallel processing for the Monte Carlo simulation offers an attractive approach toward improving the overall computational time. Parallelization of the Monte Carlo code is a straight forward approach and is based on distributing the job (number of histories) among different processors that work independently of each other in parallel. Usually, the processors are divided into two classes in this parallel computing. One is the master processor, and the others are slave processors. Because all the processors share the same target information, they do not need to communicate during the calculations, but their final results are passed to the master node when they finish their calculations. Thus, the parallel efficiency is directly proportional to the number of processors employed. The most important problem for this type of parallel processing is to generate a completely independent series of random numbers on each processor. The details for this problem were fully discussed elsewhere.[21] The structure of the PMCEPT code is the single program multiple data (SPMD) structure in the sense that the master processor controls the entire job as well as its own job. The standard message passing interface (MPI) was implemented for the communications between processors. The MPI is a standards-based message passing library for a set of processing elements, typically with distributed memory. It is also one of the most popular interfaces for parallelizing existing serial applications.

RESULTS AND DISCUSSION

Computer technologies and computational tools are essential for modern radiotherapy that requires for the accurate diagnosis of disease, design of delivery, and verification of treatment. Recently developed computer-aided technologies that fuse multiple image modalities such as CT, PET, and MRI have enabled image-guided radiotherapy, with computer simulation taking a central part. However, the safety and

appropriateness of the technology should be conformed before it is implemented for clinical use. Although Monte Carlo dose calculation codes require two highly related tasks (validation and verification) in general, validation is often folded into the verification process, which compares the calculated results with those obtained by measurements or well-proved codes, because of the complexity of the Monte Carlo codes.

The PMCEPT code is a CT-based Monte Carlo dose calculation code. The target geometry is designed as a collection of voxels in a three-dimensional cartesian coordinate system using each patient's CT image for customizing the treatment, with no reduction in resolution. The material properties in each voxel are calculated from the CT number. The density of the material in each voxel is determined from the CT number with a monotonically increasing, piecewise- continuous linear function. However, the code can also simulate an arbitrary geometry by using voxel approximation as shown in Fig. 1. Fig. 1 is a schematic accelerator head structure to show how to make a voxel from a collection of objects of arbitrary shapes. The computer aided design (CAD) technique is used to make adaptive meshes for each object and to convert their geometry information into regular Eulerian meshes (voxels). The initial beams are falling in from above along the positive Z-direction in the computational coordinate system.

1. Comparison with MCNP5

According to ICRU Report 35 (1984),[37] water is recommended as the standard medium for absorbed dose measurements because, for electron beam irradiations, the absorbed dose distributions in water and human soft tissue are very similar. Furthermore, the constant chemical composition and density of water present a distinct advantage. Thus, it is recommended that other material phantom data be converted to in-water-data for clinical uses. For this benchmark study, the shape of the target data must be the same as the available representation of the patient's data. Clinical patient geometry is obtained from computerized tomography (CT) scanning. The pixels in CT are converted to voxels that are volumes, not areas. In addition, the popular CT images can easily be converted into three-dimensional cubes or voxels by mapping the densities of the regions. In this study, the target is described in a hexahedral water phantom as having many small voxels in a three-dimensional cartesian coordinate system because it simulates the CT representation of the patient data. The standard size recommended is, as for photon and electron beams, a 30-cm cube. Such a phantom is convenient for any energy used and for most clinical situations.

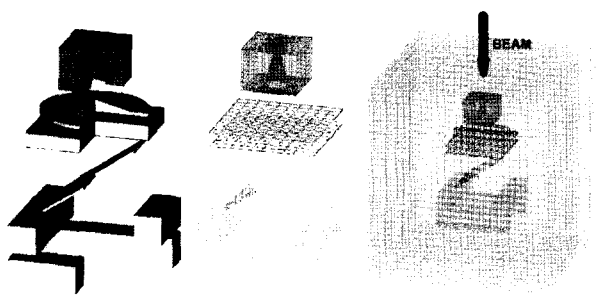

Fig. 1. Schematic accelerator head showing how to make voxels from arbitrary geometries. The adaptive meshes for each object are drawn from the mesh generation program, and the adaptive coordinate information is approximated into regular grid meshes (voxels).

We simulated two sizes of target: $10.5\times10.5\times20$ cm^3 and $30.1\times30.1\times22$ cm^3. The former is used for the evaluation of the PMCEPT code by comparing the normalized absorbed doses with those of the MCNP5, version 5 (2003), code developed by Los Alamos National Laboratory. Both absorbed doses are normalized by the maximum value of PMCEPT result. The MCNP5 code, a general purpose Monte Carlo N-Particle code, is widely used for clinical calculations in many hospitals. The latter target size is used for studying the feasibility of building a radiation treatment planning simulation system. The cell size of the former is $0.5\times0.5\times0.5$ cm^3, and that of the latter is $0.1\times0.1\times0.1$ cm^3. The numbers of voxels are 17,641 and 19,932,221, including the default medium of vacuum, respectively. The odd dimensions are used to ensure a column of voxcels on the central axis. Reference 37 describes four different principal types of radiation sources and beam geometries. Among them, the most elementary type of electron beam is the pencil beam or, more specifically, the monodirectional beam from a point source. However, we chose the plane parallel beam for this study because it describes the situations more realistically. The beam distribution area is 2.5×4.5 cm^2 in the x-y plane at z=0.0. This area is smaller than the size of the phantom. The beam is assumed to be distributed uniformly on this area. The initial kinetic energy of

each electron beam is 20-MeV. This energy corresponds to the upper bound of the clinically used electron beam radiotherapy. We chose a high energy beam for this study because the computing time, in general, increases as the initial beam kinetic energy increases, and the statistical convergence becomes slower as the beam distribution area becomes larger.

Fig. 2 shows the depth dose distributions along the central voxels. Each voxel volume in the central column is 0.5×0.5×0.5 cm^3. The two results agree within a 1 % error of the dose maximum. One million case histories were simulated for each code to achieve statistical fluctuations of about 0.2%. Fig. 3 shows the isodose curves in the y-z plane at the center of the x-axis (x=0.0) (left-hand side) and those in the x-z plane at the center of the y-axis (y=0.0) (right-hand side). The dark curves represent the PMCEPT results and the light curves the MCNP5 results. The PMCEPT results agree well with those of the MCNP5 in both figures. Moreover, the PMCEPT code was approximately twenty times faster than the MCNP5 code on an IBM ThinkPad X40 (laptop) with 1.2 GHz cpu and 512 MB ram memory operated by RedHat Linux 9.0 with an absoft Fortran compiler. Thus, the results suggest that the PMCEPT code can provide clinically acceptable and accurate solutions faster than the MCNP5 code.

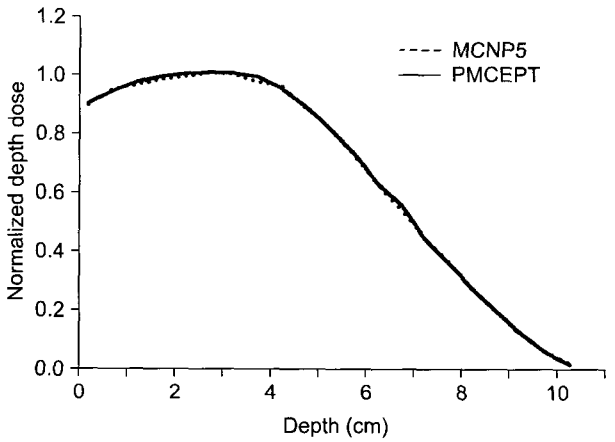

Fig. 2. Normalized depth dose distributions of the PMCEPT and the MCNP5 codes at the central column of the voxels. Both absorbed depth doses are normalized by the maximum value of the PMCEPT result.

2. Comparison with GEANT4

Photon beams of 4~25 MV energy range produced by a medical linear accelerator are commonly used in radiotherapy of tumors that occur below the skin surface. The photon beams are produced by electron beams hitting high atomic number material targets such as tungsten on the medical accelerator head. The treatment head of an accelerator includes this device (x-ray target, flattening filter, monitor unit chamber, and primary collimator) to convert the electron beam into a relatively flat, wide beam of x-ray photons. Thus, it is important to understand both the radiation transport through the head of treatment machine and the influence on the beam incident on a patient.

In general, most Monte Carlo codes use beam head profiles (phase-space files) calculated from a dedicated code such as BEAM. Therefore, in this study, we compare the PMCEPT

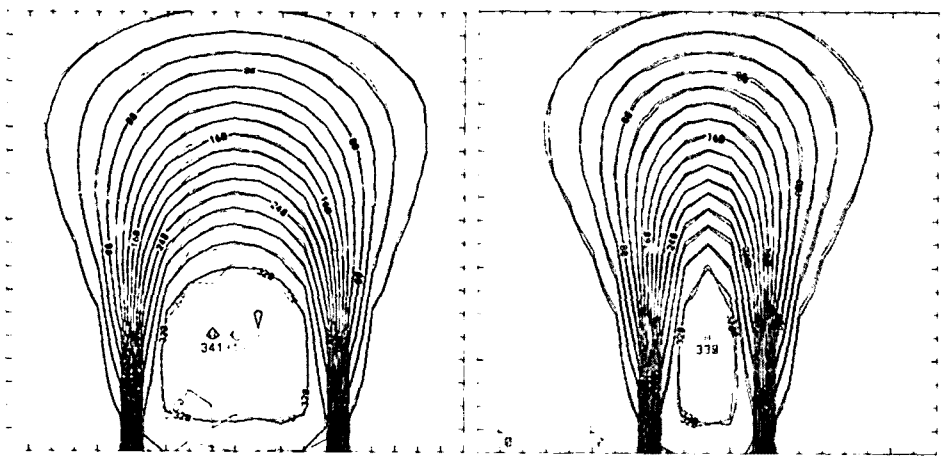

Fig. 3. Iso-dose curves in the y-z plane at x=0 (left-hand side) and in the x-z plane at y=0 (right-hand side). The light curves represent the MCNP5 results and the dark curves the PMCEPT results. The unit of dose is 10^{-12} Gy-cm^2/particle.

transport within the patient part only with that of GEANT4. GEANT4 is an object-oriented (with C++) Monte Carlo simulation toolkit that has been developed by a worldwide collaboration of scientists. It is also widely used in medical physics.

Fig. 4 shows normalized deposited depth dose curves of the PMCEPT and GEANT4 codes irradiating photons of energies of 6- and 18-MV on a water phantom. The values are normalized by the maximum of the PMCEPT result. The target size is $30.2\times30.2\times30$ cm^3, which is the recommended size by the International Commission of Radiation Units and Measurements (ICRU).

The cell size is $0.2\times0.2\times0.2$ cm^3. The deposited doses were collected in the cell size of $1\times1\times0.2$ cm^2 at the center of beam axis (z-axis). We also simulated for the beryllium phantom in the same condition. Energy cut-offs of 10-keV for electrons and 1-keV for photons were used in the calculation. Ten million broad and parallel primary photon beams were simulated and the statistical uncertainties in both targets were 0.8 % and 1.0 % for 6- and 18-MV energies, respectively. The differences between PMCEPT and GEANT4 are equal to or less than 1% of the dose maximum in both targets. The computing time of the PMCEPT code was approximately three times faster than that of GEANT4 code for the 18-MV photon

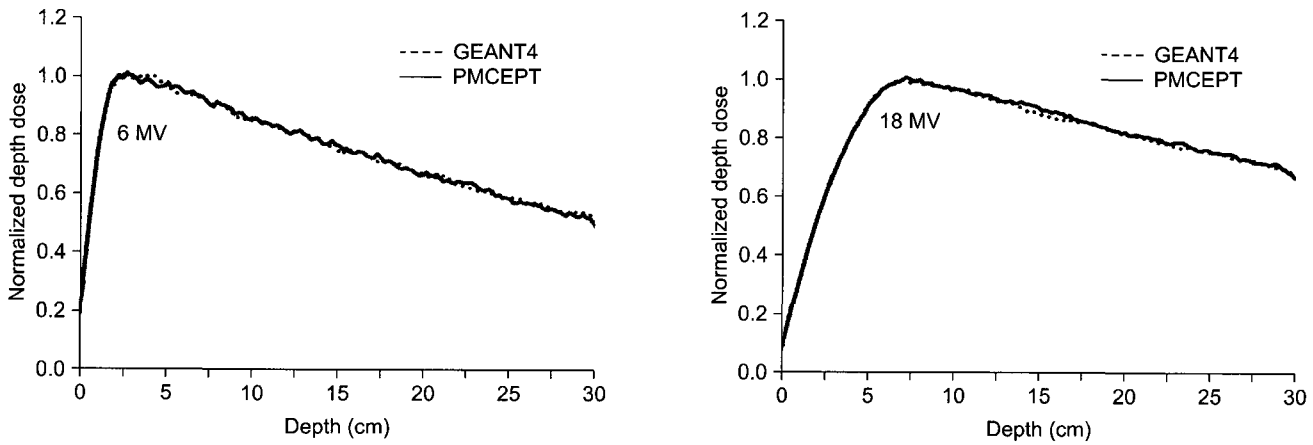

Fig. 4. Normalized depth dose distributions of the PMCEPT and the GEANT4 codes irradiating photons on the water phantom. Two energies, 6- and 18-MV are compared.

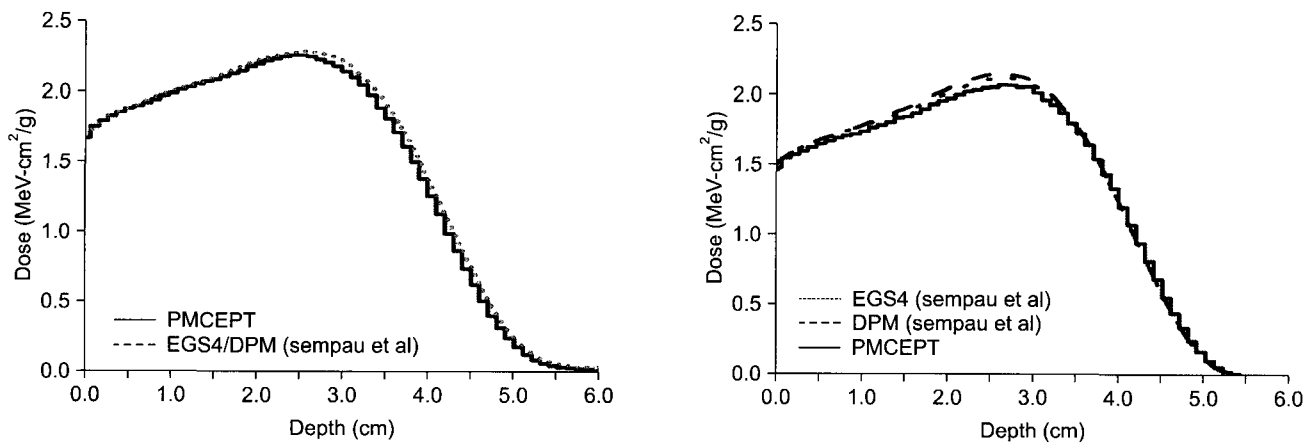

Fig. 5. Depth dose distributions in an ICRU bone phantom irradiated by a 18-MeV broad and parallel electron beam (left-hand panel) and in a water phantom irradiated by a 10-MeV broad and parallel electron beam (right-hand panel). The results are normalized by the maximum of the PMCEPT result.

beams irradiating the water phantom.

3. Comparison with EGS4 and DPM

A megavoltage linear accelerator has been the standard radiotherapy equipment for the past 20~30 years. Most megavoltage units today also have electron-beam capabilities, usually in the energy range of about 4~20 MeV. A series of high-energy electron beam benchmark simulations were also performed. Fig. 5 compares normalized depth dose distributions in semi-infinite bone (left-hand panel) and water (right-hand panel) phantoms irradiated by 18-MeV and 10-MeV broad and parallel electron beams, respectively. We have no timing benchmark results for these comparisons because the results of EGS4 and DPM are taken from reference 18. ICRU-bone and water are the most interesting materials in radiotherapy. Overall, they agree well with each other. The differences between PMCEPT, EGS4, and DPM are equal to or less than about 1.5% of the dose maximum in these simulations and the statistical uncertainty of the curves presented are on the order of 0.2% of the dose maximum. However, DPM has a bigger error at the dose maximum on the water phantom then PMCEPT and EGS4. We assume that this is due to the approximate characteristics of the DPM code.

Several multiple slab configurations were chosen to test PMCEPT with inhomogeneous geometries, and two results are presented in Fig. 6. The agreement between the PMCEPT, EGS4, and DPM codes, is excellent in both the water/bone/water and water/titanium/bone/water profiles shown in Fig. 6, with differences of about 1 % of the dose maximum, reaching a maximum of about 2% between PMCEPT and DPM for the 18-MeV electron beam.

4. Comparison with experiments

Absolute calorimetric electron dose measurements from the Sandia National Laboratories38 were compared with the results of Monte Carlo simulations performed using the PMCEPT code. These measurements are considered to be among the most accurate data ever published for electron beams with energies less than or equal to about 1.0-MeV in high atomic number media and at medium interfaces. The experimental relative error of the dose measurement was about 2~3%. As for the homogeneous media, the depth dose distributions for about 0.5-MeV and 1.0-MeV electron beams normally incident on semi-infinite aluminum and uranium targets were compared. The relevant depth dose distributions are calculated as a function of the scaled depth of z/R_0, where z is the depth in the phantom and R_0 is the electron continuous-slowing down approximation (CSDA) range which is given in each figure caption. The primary and the secondary electrons are transported down to a kinetic energy of 10-keV, and bremsstrahlung photons are generated above the threshold energy of

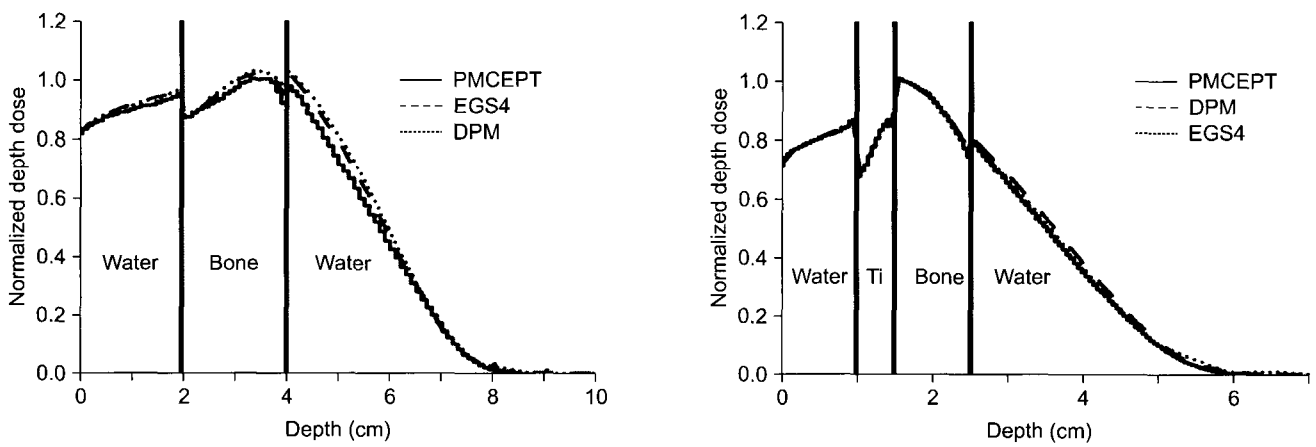

Fig. 6. Normalized depth dose distributions in a water phantom with a bone layer irradiated by a 18-MeV broad and parallel electron beam (left-hand panel) and in a water/titanium/bone/water target irradiated by a 15-MeV broad and parallel electron beam (right-hand panel). The PMCEPT results are compared with those of EGS4 and DPM codes.[18]

1-keV. Other secondaries with lower energies than these specific energies are treated as being deposited on the spot. The total number of histories was simulated until the statistical uncertainty of the simulation was on the order of 0.2% of the dose maximum for all cases. To be consistent with measurements, we use the same electron ranges which, however, are slightly different from recent evaluations. The values of the CSDA ranges for kinetic energies of 0.5-MeV, 0.521-MeV, 1.0-MeV, and 1.033-MeV and corresponding material densities are also seen elsewhere.[22]

Fig. 7 compares the normalized depth dose curves in a semi-infinite aluminum target from the PMCEPT simulation with the experimental data for broad and parallel electron beam energies of 0.521- (left-hand panel) and 1.033-MeV (right-hand panel). The absorbed doses are normalized by the maximum dose of PMCEPT and the horizontal axis is given as a unit of the CSDA range of the aluminum at the given energy. We see that both the shapes and the absolute magnitudes of the curves from the PMCEPT calculation agree well with the experimental data over the whole range, within an error of approximately 1.0%. The small fluctuations in the dose buildup region and dose maximum in the experimental data in the right-hand panel are mainly due to experimental error. The estimated experimental uncertainty is about 1.4%. Although moderate atomic number materials such as aluminum are not important ingredients of the human body, they are still important biomaterials and are sometimes used for brachytherapy, decelerators, or tissue compensators on the skin of a patient.

The multiple scattering algorithms used in simulations may affect the electron dose distributions.

The discrepancies observed in high atomic number media are often attributed to the multiple-scattering models and bremsstrahlung cross-section normalization. In general, the Molliere multiple scattering theory is known to lead to systematically lower average angular deflections in high atomic number media, especially at low energies ($<$1.0-MeV), in comparison with the more accurate Lewis's electron multiple scattering distribution[34] that is now employed in the PMCEPT code. Among the benchmark simulations in this paper, uranium has the highest atomic number, 92. The results are shown in Fig. 8. The simulated results agree well with the experimental results. Considering the facts that the multiple scattering algorithms used for most Monte Carlo codes affect dose discrepancies sensitively for high atomic number media at low energy and that the bremsstrahlung cross-sections have a greater effect for high irradiation energies, the good agreement between simulations and experiments over a wide range of atomic number targets suggests that the PMCEPT electron transport model is as accurate as the models used in other

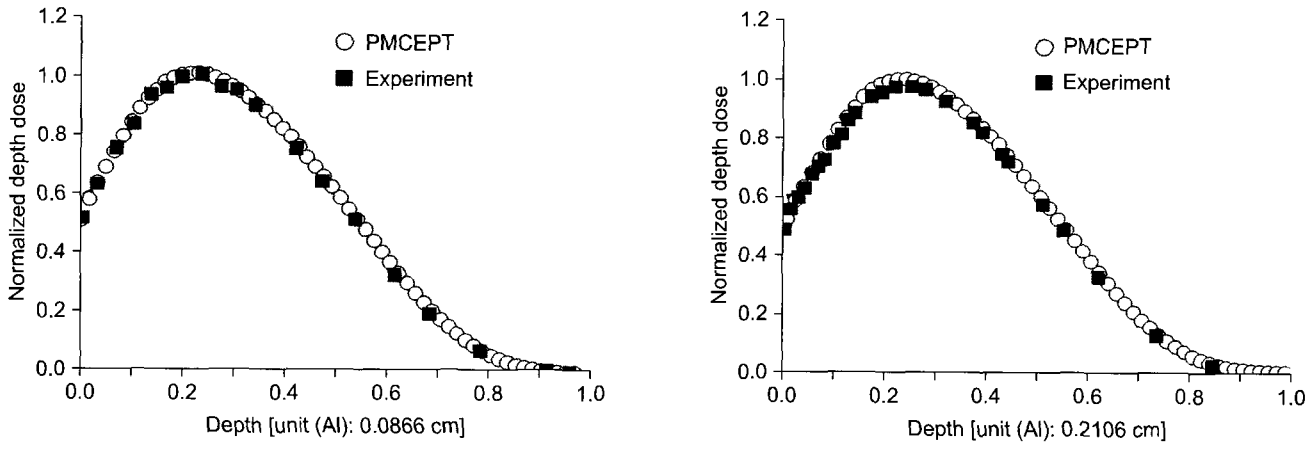

Fig. 7. Normalized depth dose distributions in semi-infinite aluminum (Z=13) irradiated by 0.521-MeV (left-hand panel) and 1.033-MeV (right-hand panel) broad and parallel electron beams. The PMCEPT results are compared with experiments. The estimated experimental[38] uncertainty is 1.4%. The statistical uncertainty of the simulations is on the order of 0.2% of the dose maximum.

well-known codes, such as MCNP5, GEANT4, EGS4, and DPM.

Exact determination of the dose distribution at medium interfaces is much more important than in the homogeneous media in radiation treatment planning because the human body is comprised of various inhomogeneities. Most previous studies compared Monte Carlo photon/electron transport codes with experiments for dose distributions in a homogeneous water or water-equivalent medium. Relatively few investigated inhomogeneities, specifically, for low energy electron dose distributions in high atomic number media and at their interfaces. Specifically, exact dose estimates at medium interfaces frequently required in radiotherapy may include tissue/bone/high-atomic-number-media interfaces, for example, brachytherapy. Accurate interface dosimetry remains a challenge in spite of the many simulations and measurements carried out over the last 30 years. Fig. 9 compares the PMCEPT-calculated dose distributions with the calorimetric measurement experiments for the cases of 0.521- (left-hand panel) and 1.033-MeV (right-hand panel) electron beams normally incident on Ta/Al con-

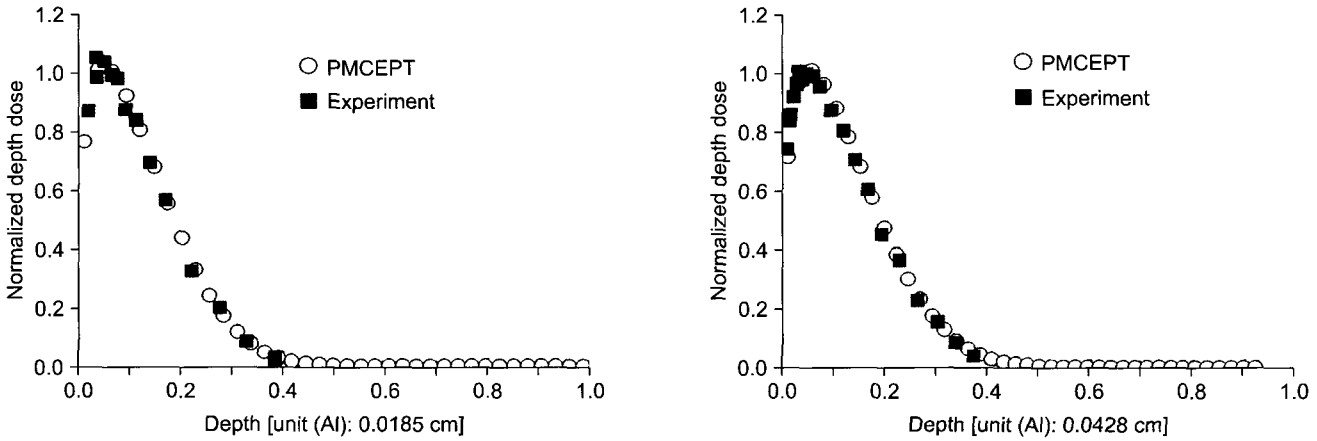

Fig. 8. Normalized depth dose distributions in semi-infinite uranium (Z=92) irradiated by 0.5-MeV (left-hand panel) and 1.0-MeV (right-hand panel) broad and parallel electron beams. The PMCEPT results are compared with experiments. The estimated experimental[38] uncertainty is 1.4%. The statistical uncertainty of the simulations is on the order of 0.2% of the dose maximum.

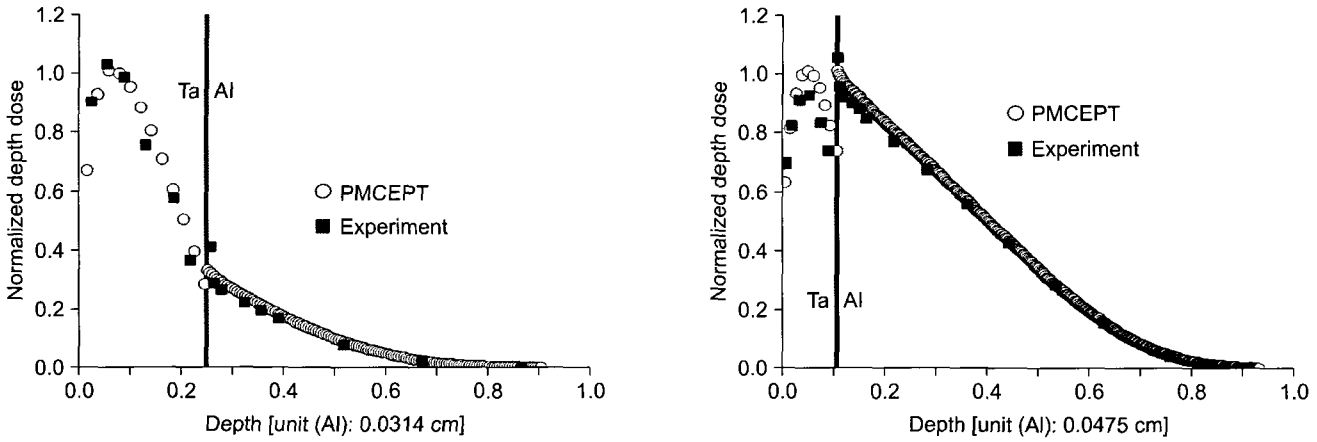

Fig. 9. Normalized depth dose distributions in a tantalum/aluminum configuration irradiated by 0.521-MeV (left-hand panel) and 1.033-MeV (right-hand panel) broad and parallel electron beams. The PMCEPT results are compared with experiments. The estimated experimental[38] uncertainty is 1.2% in Ta and 1.4% in Al. The statistical uncertainty of the simulations is on the order of 0.2% of the dose maximum.

figuration. This is a typical example of a high-atomic number/low-atomic-number interface. Electronic equilibrium is usually lost at interfaces for heterogeneous media. The agreement between simulation and experiment is reasonably good for the Ta/Al profile although there is a small deviation (approximately 2~3% error) in the low atomic number material near the medium interface. Thus, the result suggests that the PMCEPT code is quite accurate when simulating electron boundary crossings between two media with large differences in both atomic number and density.

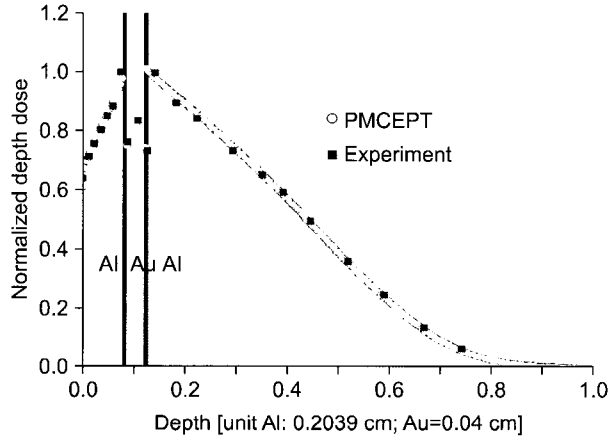

Fig. 10. Normalized depth dose distributions in an aluminum/gold/aluminum configuration irradiated by a 1.0-MeV broad parallel electron beam. The PMCEPT results are compared with experiments. The estimated experimental[38] uncertainty is 1.4% in Al and 1.5% in Au. The statistical uncertainty of the simulations is on the order of 0.2% of the dose maximum.

Fig. 10 shows the results for a three-layered low-atomic-number/high-atomic-number/low atomic-number phantom. As shown in the figure, an approximately 0.02 mm thick layer of gold (high atomic number) is sandwiched between two layers of much lower atomic number materials. The thickness of the low atomic number material in front of the gold was carefully chosen so that the dose maximum would occur in the gold. The thickness of the low atomic number layer behind the gold was chosen to be thicker than the continuous-slowing-down approximation (CSDA) range of the normally incident 1.0-MeV electron beam. The estimated uncertainty in the measured data was approximately 1.5%, and the estimated statistical standard errors in the Monte Carlo results were approximately 0.2% at the dose maximum. Agreement between the PMCEPT and experimental results is excellent in this heterogeneous phantom. With the Monte Carlo simulation, another important concern at the medium interfaces is the boundary crossing algorithm in relation to the multiple-scattering algorithm. Any inaccuracies introduced by the approximation may be more serious for internal boundaries than for the vacuum interfaces at escape boundaries. In general, the observed discrepancies between simulation and experiment are related to the approximation that must be invoked at the material boundaries in the heterogeneous media. The PMCEPT code uses the single-scattering algorithm for the boundary crossing, which should remove the inaccuracy in the boundary crossing. The single-scattering Monte Carlo algorithm can handle the crossing of material boundaries quite rigorously. The details about

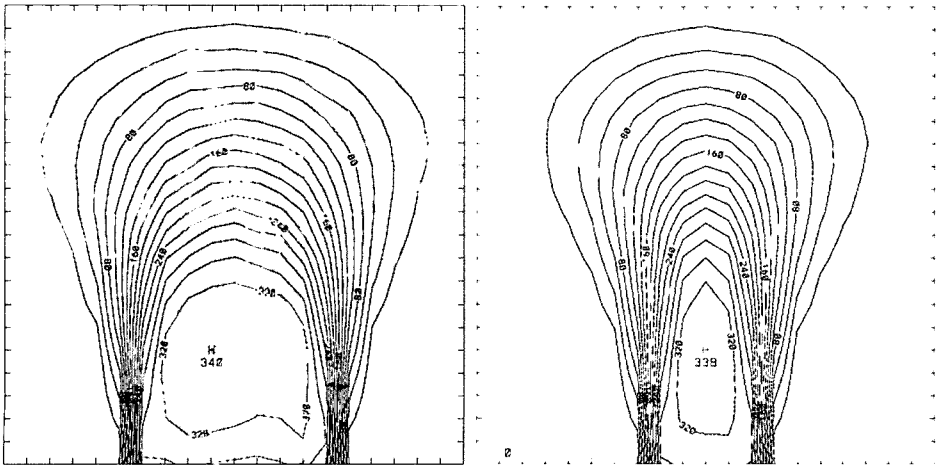

Fig. 11. Isodose curves in the y-z plane at x=0 (left-hand panel) and in the x-z plane at y=0 (right-hand panel). The light curves represent the serial results and the dark curves the parallel results using 10 processors. The unit of dose is 10^{-12} Gy-cm^2/particle.

when and how to invoke the single-scattering algorithm are explained in reference 21. We also sub-zoned the material layers into equal increments with widths of approximately 0.007 mm to make three zones in the thin gold layer. This target profile actually proved that an optimal use of a boundary-crossing index that invoked a single-scattering process solved this problem correctly although the thin zone led to excessive use of boundary crossing, resulting in longer computing time.

5. Parallel results and speedup

The parallel results calculated from ten processors were compared with the serial results for a water phantom. We compared the lateral dose distributions in Fig. 11 because the lateral distributions are more sensitive than those of depth dose. Fig. 11 shows isodose curves in the y-z plane at x=0 (left-hand panel) and in the x-z plane at y=0 (right-hand panel). The light curves represent the serial results and the dark curves the parallel results. The unit of the dose is 10^{-12} Gy-cm^2/particle. The maximum dose points agreed as shown on the left-hand panel though there was a slight difference, in part, on the next maximum isodose curve. The agreement was perfect in the x-z plane shown in the right-hand panel. One million primary case histories were simulated and the statistical error was on the order of 0.2%. The parallel speedup resulting from N processors is defined as the ratio of the serial run-time to the average run-time of the N-processors. We used the elapsed time (wall-clock time) in this study. The parallel efficiency approached 100%, as was expected, for the Linux Beowulf PC cluster, which is the most economical high-performance computer.

CONCLUSIONS

We verified a parallel Monte Carlo dose calculation algorithm (PMCEPT code) for simulations in medical physics. PMCEPT takes advantage of new transport mechanisms and accurate multiple-scattering algorithms derived from the exact Lewis's formalism.[34] The absorbed dose calculations agreed with those of the MCNP5 code within an error on the order of 1.0% for electron beams, but with a significant increase in computational efficiency. It was twenty times faster than MCNP5. The deposited depth dose curves for the photon beams agreed with those of the GEANT4 code within an error on the order of 1.0%. PMCEPT was three times faster than GEANT4. For the rigorous benchmarks, the predictions of the PMCEPT code in homogeneous and multilayered media exposed to low energy electron beams ($\leq$1.033-MeV) were compared to dose measurements. The agreement between the PMCEPT results and experiments for both homogeneous and heterogeneous media was good, with differences on the order of 1~3% of the dose maximum, reaching a maximum of 3.0% at the high-atomic-number/low-atomic-number interface. For high energy electron sources ranging from 10-MeV to 20-MeV, the popular energy range used in modern megavoltage radiation treatment, good agreement was found between the PMCEPT, EGS4, and DPM codes in homogeneous and heterogeneous phantoms, with differences on the order of 1~2% of the dose maximum. The parallel efficiency approached 100%.

Because of the fast development of computer technologies and computational tools, much more accurate Monte Carlo-based radiation treatment planning systems are replacing the system based on a simpler analytic approximation to the solution of the transport equation. This study showed that the

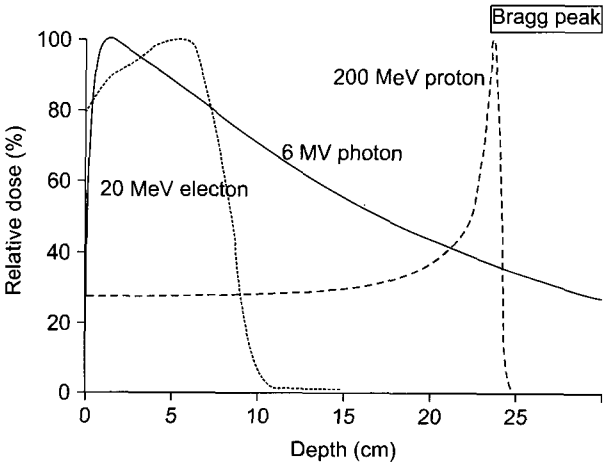

Fig. 12. Relative depth dose curves for 20-MeV electron, 6-MeV photon, and 200-MeV proton beams are compared with each other against a water phantom. The typical beam characteristics are seen. Note that proton beam shows a moderate entrance dose, followed by a Bragg peak with essentially zero dose beyond the Bragg Peak.

PMCEPT code adequately provides both fast and accurate simulation of the transport of electron and photon in CT geometry. Moreover, with the development of the proton beam accelerator, a proton beam transport algorithm is also investigated to take advantage of Bragg peak effects and the drastic fall off characteristics beyond the Bragg peak as shown in Fig. 12.

REFERENCES

1. **Chibani O, Li XA**: Monte Carlo dose calculations in homogeneous media and at interfaces: a comparison between GEPTS, EGSnrc, MCNP, and measurements. Med Phys 29: 835-847 (2002)
2. **Siantar CLH, Walling RS, Daly TP, et al**: Description and dosimetric verification of the PEREGRINE Monte Carlo dose calculation system for photon beams incident on a water phantom. Med Phys 28:1322-1337 (2001)
3. **Bortfeld T**: IMRT: a review and preview. Phys Med Biol 51: R363-R379 (2006)
4. **Cheng CW, Das IJ**: Treatment plan evaluation using dose-volume histogram (DVH) and spatial dose volume histogram (zDVH). Int J Radiat Oncol Biol Phys 43:1143-1150 (1999)
5. **Rogers DWO**: *Fifty years of Monte Carlo simulations for* medical physics. Phys Med Biol 51:R287-R301 (2006)
6. **Nelson WR, Hirayama H, Rogers DWO**: The EGS4 code system-Report. SLAC-265, (Stanford Linear Accelerator Center, Stanford, CA (1985)
7. **Berger MJ, Seltzer SM**: ETRAN, Monte Carlo code system for electron and photon transport through extended media, RISC computer code package CCC-107. Oak Ridge National Laboratory, Oak Ridge, TN, (1973)
8. **Goosens M, Giani S, Ravndal S**: GEANT: detector description and simulation tool. Technical Report CERN Program library, long writeup W5013 CERN, Geneva, Switzerland, 1993
9. **Briesmeister JF**: *MCNP - A general Monte Carlo N-Particle transport code*. Los Alamos National Laboratory Report, LA-12625-M (1993)
10. **Salvat F, Fernandez-Varea JM, Baro J, Sempau J**: PENELOPE, an algorithm and computer code for Monte Carlo simulation of electron-photon showers. in Clemat (Centro de Investigaciones Energeticas, Medioambientalesy Technologicas), Reprot No. 799 (1992)
11. **Halblieb JA, Mehlhorn TA**: ITS: the integrated TIGER series of coupled electron/photon Monte Carlo transport codes, Sandia National Laboratory report, SAND 84-0573 (1984)
12. **Fasso A, Ferrari A, Sala PR**: Electron-photon transport in FLUKA: Status. in Proceedings of the Monte Carlo 2000 conference, Lisbon, Portugal, edited by Kling A, Barao FJC, Nakagawa M, Tavora L, and Vaz P. (Springer-Verlag, Berline 2000), pp. 159-164
13. **Ma CM, Li JS, Pawlicki T, Jiang SB**: MCDOSE-a Monte Carlo dose calculation tool for radiation therapy treatment planning, in Proceedings of the XIII International Conference in the Use of Computer in Radiation therapy (ICCR), edited by Schlegel W. and Bortfeld T, (Springer-Verlag, Heidelberg, 2001), pp. 123-125
14. **Kawrakow I**: VMC++, electron and photon Monte Carlo calculations optimized for radiation treatment planning. in Advanced Monte Carlo for radiation Physics. Particle Transport Simulation and Applications: Proceedings of the Monte Carlo 2000 Meeting, Lisbon, edited by Kling A, Barao F, Nakagawa M, Tavora L, and Vaz P, (Springer, Berlin, 2001), pp. 229-236
15. **Fippel M**: Fast Monte Carlo dose calculation for photon beams based on the VMC electron algorithm. Med Phys 26:1466-1475 (1999)
16. **Wang L, Chui CS, Lovelock M**: A patient-specific Monte Carlo dose-calculation method for photon beams. Med Phys 25:867-878 (1998)
17. **Neuenschwander H, Mackie TR, Reckwerdt PJ**: MMC-a high-performance Monte Carlo code for electron beam treatment planning. Phys Med Biol 40:543-574 (1995)
18. **Sempau J, Wilderman SJ, Bielajew AF**: DPM, a fast, accurate Monte Carlo code optimized for photon and electron radiotherapy treatment planning dose calculation. Phys Med Biol 45:2263-2291 (2000)
19. **Keal PJ, Hoban PW**: Super-Monte Carlo: a 3D electron beam dose calculation algorithm. Med Phys 23:2023-2034 (1996)
20. **Kum O**: Development of web-based customized cancer radiation treatment planning simulation system (abstract). Med Phys 33: 2086-2087 (2006)
21. **Kum O, Lee S**: Development of a parallel electron and photon transport code (PMCEPT) I: method and absorbed dose computation in water. J Korean Phys Soc 47:716-725 (2005)
22. **Kim H, Kum O**: Development of a parallel electron and photon trans-port code (PMCEPT) II: absorbed dose computation in homogeneous and heterogeneous media. J Korean Phys Soc 49:1640-1651 (2006)
23. **Kum O**: Monte Carlo dose calculation in homogeneous and heterogeneous media: A comparison between the PMCEPT code and MCNP5, EGS4, DPM codes, and experiments (abstract). Med Phys 33:2122-2122 (2006)
24. **MPI Document Group**: MPI-2: message passing interface. http://www-unix.mcs.anl.gov/mpi, 2004
25. **Jeraj R, Keall PJ, Ostwald PM**: Comparisons between MCNP, EGS4 and experiment for clinical electron beams. Phys Med Biol 44:705-717 (1999)
26. **Frass BA, Smathers J, Deye J**: Summary and recommendation of a National Cancer Institute workshop on issues limiting the clinical use of Monte Carlo dose calculation algorithms for megavoltage external beam radiation therapy. Med Phys 30: 3206-3216 (2003)
27. **Jeraj R, Kowalok ME, Titz B**: Computational benchmarks for medical physics. in Proceedings of the Computational Medical Physics Working Group Workshop I: CMPWG I

ORNL/TM-2006/7, Compiled by Kirk BL. and Rice AF, 2006, pp. 5-12

28. **Mejaddem Y, Belkić Dz, Brahme A, Hyödynma S**: Development of the electron transport theory and absorbed dose computation in matter. Nucl Instr Meth in Phys Res B 187:499-524 (2002)
29. **Motz JW, Olsen HA, Koch HW**: Pair production by photons. Rev Mod Phys 41:581-639 (1969)
30. **Butcher JC, Messel H**: Electron number distribution in electron-photon showers in air and aluminum absorbers. Nucl Phys 20:15-128 (1960)
31. **Storm E, Israel HI**: Photon cross sections from 1-keV to 100-MeV for elements Z=1 to Z=100. Atom Data Nucl Data Tables 7:565-681 (1970)
32. **Klein O, Nishina Y**: Über die streuung von strahlung durch freie elektronen nach der neuen relativistischen quantendynamik von Dirac. Z für Physik 52:853-868 (1929)
33. **Berger MJ**: Monte Carlo calculation of the penetration and diffusion of fast charged particles. in Method in Computational Physics, Vol. I, edited by Alder B, Fernback S, and Rotenberg M. (Academic Press, New York, 1963)
34. **Lewis HW**: Multiple scattering in an infinite medium. Phys Rev 78:526-529 (1950)
35. **Koch HW, Motz JW**: Bremsstrahlung cross section formulas and related data. Rev Mod Phys 31:920-955 (1959)
36. http://phys.nist.gov/cgi-bib/Star.
37. **ICRU Report No. 35**: *Radiation Dosimetry: Electron Beams with Energies Between 1 and 50 MeV.* Bethesda, Maryland, International Commission of Radiation Units and Measurements (1984)
38. **Lockwood GJ, Ruggles LE, Miller GH, Halbleib JA**: Calorimetric measurement of electron energy deposition in extended media-theory vs experiment, Report No. SAND79-0414, Sandia National Laboratory, 1980

의학물리 분야에 사용하기 위한 PMCEPT 몬테카를로 도즈계산용 코드 검증

경북대학교 전자전기컴퓨터학부

금 오 연

환자의 CT자료를 기반으로 만들어진 3차원상의 표적물질에 전자 및 광자의 전달 현상을 계산하는 몬테카를로(MC) 도즈계산용 병렬프로그램 (PMCEPT 코드)을 개발하여 베어울프 PC 클러스터에 탑제하였다. 시뮬레이션에서 오차를 최소화하고 코드를 더욱 발전시키기 위해서는 현재의 MC 코드의 한계를 아는 것이 매우 유익하다. 이러한 관점에서 저자는 PMCEPT코드를 이용하여 이질 혹은 동질의 표적물질에서 표준화된 깊이 도즈를 계산하여 잘 알려진 다른 코드들, MCNP5, EGS4, DPM, GEANT4 및 실험결과와 비교를 하였다. PMCEPT 결과는 이질 혹은 동질의 표적에서 다른 코드들과 1~3% 오차 범위 안에서 잘 일치하였다. 계산시간 비교에 있어서도 PMCEPT 코드가 MCNP5 보다는 약 20배, GEANT4 코드 보다는 약 3배 정도 빨랐다. 이러한 결과를 종합하면, PMCEPT코드는 의학물리분야의 시뮬레이션 코드로 사용하기에 매우 좋은 것으로 사료된다.

중심단어: PMCEPT, 몬테카를로, 동질 및 이질 팬텀, 표준깊이도즈, 계산시간 비교